Mammalian Pitrilysin: Substrate Specificity and Mitochondrial Targeting†

K. Martin Chow,‡ O. Gakh,§ I. C. Payne,‡ Maria Aparecida Juliano,|| Luiz Juliano,|| G. Isaya,§ and Louis B. Hersh*,‡

Department of Molecular and Cellular Biochemistry, University of Kentucky, B283 BBSRB, 741 South Limestone Street, Lexington, Kentucky 40536-0509, Department of Pediatric & Adolescent Medicine and Biochemistry and Molecular Biology, Mayo Clinic and Foundation, Rochester, Minnesota 55905, and Department of Biophysics, Escola Paulista de Medicina, Sao Paulo, Brazil 04044-20

Received August 26, 2008; Revised Manuscript Received February 4, 2009

ABSTRACT: The substrate specificity of the mitochondrial metallopeptidase proteinase 1 (MP1) was investigated and its mitochondrial targeting signal identified. The substrate specificity of MP1 was examined with physiological peptides as substrates. Although the enzyme exhibits broad substrate specificity, there is a trend for peptides containing 13 or more residues to exhibit K_m values of 2 μM or less. Three of four peptides containing 11 or fewer residues exhibited K_m values above 10 μM. Similarly, peptides containing 13 or more residues exhibited k_{cat} values below 10 min^{-1}, while three of four peptides containing 11 or fewer residues exhibited k_{cat} values above 30 min^{-1}. Many of the peptide cleavage sites of MP1 resemble that of the mitochondrial processing protease (MPP); however, MP1 does not process the precursor form of citrate synthase. The enzyme, however, does cleave the released prepeptide from precitrate synthase. A mitochondria localization was shown in MP1 transfected NT2 and HepG2 cells. Deletion of the N-terminal 15 amino acids caused MP1 to be mislocalized to the cytoplasm and nucleus. Furthermore, when fused to green flourescent protein, this 15-amino acid N-terminal sequence directed the fusion protein to the mitochondria.

Zinc-dependent peptidases of the M16 family possess the active site motif HEXXH, in which the two histidine residues coordinate a zinc atom and the glutamate facilitates the attack of a water molecule on the scissile bond. A subgroup of the M16 family of metallopeptidases contains an inverted Zn-binding motif HXXEH, and these peptidases are referred to as inverzincins (*1*). The first identified inverzincin was pitrilysin protease III (*2*), a gene product of the *ptr* gene in *Escherichia coli*.

Besides protease III (EC 3.4.24.55), several mammalian inverzincins have been identified and classified as M16A family members (*3*). These include insulysin (insulin degrading enzyme, IDE, EC 3.4.24.56) and nardilysin (NRDc, EC 3.4.24.61). Both protease III and insulysin exhibit a broad substrate specificity cleaving a variety of peptides. The structures of pitrilysin protease III and insulysin (*4*) are very similar and appear to be "clam-shaped" with the insulysin structure in a closed conformation and the protease III structure in an open conformation. The closed conformation tightly locks down the substrate in the interior of the enzyme, requiring a conformational change to permit product release. This conformational change is likely the rate-limiting step for the insulysin reaction. Both of these enzymes have an active site pocket that can accommodate and interact with a variety of peptides, explaining in part their broad substrate specificity. In contrast, nardilysin has a more defined substrate specificity, cleaving peptides primarily at or between dibasic pairs (*5*).

In terms of cellular functions, insulysin has been implicated in regulating insulin and amyloid β-peptide levels and thus has been linked to diabetes and Alzheimer's disease (*6, 7*). Furthermore, insulysin is up-regulated in activated macrophages (*8*) and some T cells (*9*) where its ability to cleave β-endorphin suggests a role in modulating immune function. Nardilysin has been implicated in regulating reproduction (*10*) and cell cycling (*11*) and increasing the efficiency of energy metabolism (*12*). It has also been described as a surface receptor (*13*) and as an interacting protein for the PIP4 binding protein (*14*). The function of protease III remains unclear since there is no discernible phenotype detected in mutant *ptr*.

The mitochondrial processing peptidase (MPP, EC 3.4.24.64) has been classified as an M16B subfamily member. MPP plays an important role in the processing of nuclear encoded proteins as they enter the mitochondria. The cleavage of the presequence signal of the mitochondrial precursor proteins by MPP is an important step preceding folding and subsequent maturation of the precursor polypeptides. Except in plants, MPP is a heterodimeric enzyme with the Zn-binding motif located in β-MPP. As for the cleavage specificity of MPP, Arg is often found two or three residues at the amino side of the scissile bond. This specificity has been referred to as R-2 or R-3 motifs, respectively (*15, 16*).

* To whom correspondence should be addressed. Phone: (859) 323-5549. Fax: (859) 323-1727. E-mail: lhersh@uky.edu.

† This research was supported by grants from the National Institute on Drug Abuse, Grant DA 02243, and from the National Center for Research Resources (NCRR), Grant P20RR02017.

‡ University of Kentucky.

§ Mayo Clinic and Foundation.

|| Escola Paulista de Medicina.

10.1021/bi8016125 CCC: $40.75
Published on Web 02/05/2009

However, it is unclear how MPP makes a single and specific cleavage on preproteins that have very dissimilar presequences.

Mammalian metallopeptidase 1 (MP1; ref *17*) and presequence peptidases (PrePs) in *Arabidopsis thaliana* are the newest inverzincin family members and are included in an M16C subfamily. PrePs are located in both mitochondria and chloroplast (*18*). The function of PrePs is thought to involve the clearance of presequences that are derived from mitochondria precursor protein cleavage by MPP. Evidence that MP1 is also localized in mitochondria has been described (*19, 20*); however, a mitochondrial targeting sequence has not been identified or characterized. On the basis of sequence similarity and subcellular localization, MP1 may have a similar function as the PrePs. MP1 was originally described on the basis of its ability to cleave the $T^{13}-R^{14}$ bond of leumorphin (dynorphin B-29); however, there have not been any further studies on its substrate specificity. Furthermore, MP1 may have additional functions associated with tissue remodeling, as the expression of MP1 is up-regulated upon nuclear transplantation in mouse embryonic stem (ES) cells (*21*). The present study was designed to further characterize MP1 in terms of its substrate specificity and mitochondrial targeting.

EXPERIMENTAL PROCEDURES

Materials. An antibody against the sequence (^{753}AEMTDIKPILRKLPRIKK) of human MP1 was raised in a rabbit by Bethyl Laboratory (Montgomery, TX). The monoclonal antiflag antibody M2 was purchased from Sigma-Aldrich. Anti-Lamp1, anti-calnexin, and anti-cytosolic thiolase were generously provided by Dr. S.W. Whiteheart (University of Kentucky). Polyclonal rabbit anti-mitochondrial malate dehydrogenase (mMDH) was a generous gift from Dr. Arnold W. Strauss (Vanderbilt University). Secondary florescent antibodies to mouse and rabbit were purchased from Vector Laboratories (Burlingame, CA). Poly-L-lysine was from Sigma-Aldrich. Recombinant yeast mitochondrial processing protease (yMPP) was expressed in *E. coli* and purified as previously described (*22*). The citrate synthase (CS) presequence peptide (MALLTAAARLFGAKNASCLVLAARHAS-NH_2) was synthesized by the W. M. Keck Foundation Biotechnology Resource Laboratory (New Haven, CT). Dynorphin B and β-endorphin were purchased from neoMPS (San Diego, CA) and dynorphin A and Leu-enkaphalin from Bachem (Torrance, CA), and the rest of the peptides used in this study were from California Peptide Research (Napa, CA).

Complementary DNA (cDNA) Subcloning. A cDNA clone for human MP1 (accession no. BC005025) was purchased from Invitrogen. The cDNA was subcloned into the pFastbac 1 cloning vector (Invitrogen) and used in the Bac-to-Bac expression system to generate baculovirus. The 5′ 416 base pairs were amplified and introduced into a Bam H1 site of pFastbac 1 by a polymerase chain reaction (PCR) using the following forward and reverse primers, respectively: 5′-TCT GGA TCC CAC CAT GTG GCG CTG C-3′ (BamH1 site underlined) and 5′-TTC ATG AAC GTG GAG AGG GAC-3′. This PCR product contains a Bam H1 and an internal Age I site. The remaining cDNA fragment was excised from the original clone with 5′-Age I and 3′-Xho1. These two fragments were then ligated into the pFastbac 1 vector.

For subcellular localization studies, the full-length MP1 cDNA was subcloned into the mammalian expression vector pcDNA3.1 (Invitrogen) with the following modification. The stop codon was removed, and an oligonucleotide encoding a flag epitope sequence followed by a stop codon (5′-TGT CCT CGA GTC ACT TAT CGT CGT CAT CCT TGT AAT CTC GGA TGA TCC AG-3′) (Xho1 site and stop codon underlined) was added to the 3′-end of the cDNA. To determine the mitochondrial targeting signal, two N-terminal truncation mutants MP1Δ15 and MP1Δ38 were constructed by PCR using the following forward primers: 5′-CAT AGG ATC CAT GAG CGG CGG ACA-3′ (MP1Δ15) and 5′-CAT AGG ATC CAT GCA GTA TAA ACT A-3′ (MP1Δ38), which contain a start codon preceded by a BamH 1 site. The reverse primer and the subsequent cloning procedures were the same as the above-mentioned method of cloning MP1 into pFastbac 1.

Expression and Purification of MP1. Baculovirus expressing MP1 was prepared according to the manufacturer's instructions and used to infect Sf9 cells. Three days post-transfection, cells were collected by centrifugation at 2000*g* for 10 min and then frozen at −80 °C until use. The cell paste was suspended in 10 volumes of 20 mM Tris buffer at pH 7.5 and sonicated with a Branson Sonifier 450 (output control at 4, duty cycle 30%, 10 s for three times). The homogenate was centrifuged 30 min at 30 000*g* and the supernatant applied to Waters Acell Plus QMA anion exchange column (15 mL) in 20 mM Tris buffer at pH 7.5. Proteins were eluted with a 0−0.5 M linear NaCl gradient with MP1 eluting at ∼0.2 M NaCl. The eluted enzyme was concentrated and applied to a Pharmacia Superdex 200 column (1.6 cm × 60 cm), equilibrated, and run with 20 mM Tris buffer at pH 7.5. Lastly the enzyme was chromatographed on a 1 mL Pharmacia Mono Q column in the 20 mM Tris buffer and eluted with a linear salt gradient. The active MP1 fractions were pooled, desalted, concentrated with a Millipore Centricon concentrator, and stored in 20% glycerol at −80 °C. The purified enzyme appeared essentially homogeneous as judged by sodium dodecyl sulfate polyacrylamide gel electrophoresis (SDS-PAGE; Figure 1a). The form of MP1 isolated by this method is processed at its N-terminus as determined by its molecular size and its mitochondrial location.

MP1 was also expressed in *E. coli* as a glutathione-S-transferase (GST) fusion protein using the pGEX-5X expression vector. A tobacco etch virus (TEV) protease cleavage site followed by a BamH1 restriction site in frame with the MP1 cDNA was subcloned into the pGEX-5X vector. The construct pGEX-GST-TEV-MP1 was transformed into the *E. coli* strain BL-21(DE3), and cells were grown at 37 °C until an OD_{600} of 0.5−0.7 was reached. Expression was induced by the addition of isopropy-β-D-thiogalactoside to a final concentration of 0.5 mM. Induction was carried out overnight at room temperature. Cells were harvested and washed with phosphate buffered saline (PBS). Cell pellets were suspended in 25 mM potassium phosphate buffer at pH 7.5 containing 1 mM phenylmethylsulfonylfluride and 10 μM E-64, broken with a French press, and centrifuged at 30 000*g* at 4 °C for 30 min. The supernatant was passed through a glutathione agarose column (Invitrogen) and washed with the same buffer without protease inhibitors. The fusion protein was eluted with 15 mM glutathione and

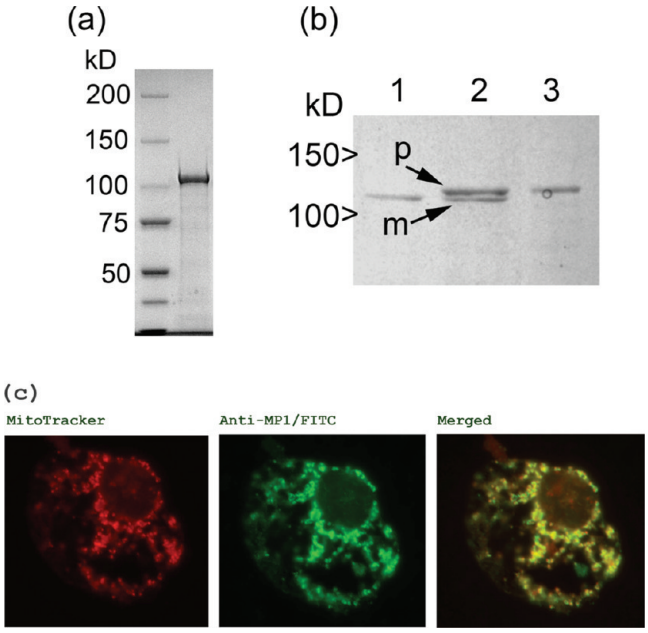

FIGURE 1: Recombinant human MP1 from Sf9 insect cells is processed. (a) Purity of recombinant human MP1 derived from Sf9 cells. Recombinant MP1 (2 μg), purified as described in Experimental Procedures, was analyzed by SDS-PAGE on a 7.5% gel. Left lane shows the All Blue (BioRad) molecular weight standard. (b) Molecular weight comparison between purified MP1 from Sf9 cells and from *E. coli.* Lane 1, purified MP1 from Sf9 cells; lane 2, purified MP1 from Sf9 cells and from *E. coli* mixed; lane 3, purified MP1 from *E. coli*. The recombinant precursor form of MP1 (p) is processed to the mature form (m) in Sf9 cells. (c) Subcellular localization of MP1 in Sf9 cells. MP1 was detected with a rabbit anti-MP1 antibody and colocalized with MitoTracker (Invitrogen; see Experimental Procedures).

cleaved with TEV protease (*23*). MP1 and GST were separated on an S-200 gel filtration column. The MP1 formed by this process contains the full-length unprocessed form of MP1 with two additional amino acids, Gln-Pro, at its N-terminus.

Assay of MP1 Activity. MP1 activity was routinely assayed in 25 mM potassium phosphate buffer at pH 7.5 using the fluorogenic peptides Abz-RRQFKVVTRSQ-EDDnp[1] and Abz-GGYRRGQ-EDDnp (Abz/Dnp peptides) as described (*5*). Hydrolysis of physiological peptides was determined by following their disappearance at 214 nm by reverse phase high-performance liquid chromatography (HPLC) on a Phenomnex C_{18} column (5.0 × 4.6 mm). Peptides were separated by a linear gradient from 0.1% trifluoroacetic acid in 90% water/10% acetonitrile to 0.1% trifluoroacetic acid in 50% water/50% acetonitrile. The k_{cat} values were determined based on the rate observed at 5% or less hydrolysis of a physiological peptide at a saturating concentration and using a molecular weight of 117 kDa for MP1. The K_m of physiological peptides was determined by using them as alternate substrate inhibitors of Abz-GGYRRGQ-EDDnp hydrolysis over the range of $0.5K_m$ to $2K_m$ with five to seven peptide concentrations used. Data were analyzed by Dixon plots with Graphpad Prism software (Graphpad, San Diego). Other kinetic parameters were determined by fitting to the Michaelis−Menten equation with the same software. Standard errors were 10% or less.

Identification of Peptide Cleavage Products. Physiological peptides were incubated with MP1 for various times to establish the order of product appearance. Cleavage products were separated by reverse phase HPLC on a Vydac C_4 column (*5*). In the case of ANP and somatostatin, the peptides were reduced and carboxymethylated prior to HPLC analysis. Peptides or their reaction products were collected manually, freeze-dried, and identified by mass spectrometry using a Bruker Autoflex time-of-flight mass spectrometer with α-cyano-4-hydroxycinnamic acid as the matrix or on a ThermoFinnigan LCQ, with sample introduction by direct infusion. These analyses were performed at the University of Kentucky Mass Spectrometry Core Facility.

Cell Culture. HepG2 cells were grown in F12/minimum Eagle's essential medium containing 10% iron-supplemented bovine calf serum (Atlanta Biological, Atlanta, GA). NT2 cells (ATCC# CRL-1973) were grown in Dulbecco's modified Eagle medium containing 10% fetal calf serum, 4.5 g of glucose per liter, and 1% glutamine (Gibco). Penicillin/streptomycin (Gibco; 1%) was included in all media. Cells were kept at 37 °C and 5% CO_2. The FuGENE 6 reagent (Roche) was used for cell transfections. The DNA to reagent ratio was 1 μg per 3 μL of FuGENE 6 using a total of 6 μg of DNA per 10 cm culture dish. Cells were harvested 48 h after transfection. For Sf9 cells, baculovirus containing the full-length MP1 was used. Virus obtained from the second round of amplification was diluted 10 times with Sf-900 II SFM (Invitrogen) and applied directly to Sf9 cells. Immunocytochemistry was performed after 2−3 days of incubation.

Immunocytochemistry. Cells were plated on polylysine coated coverslips and transfected 12−24 h later. Cells were washed with PBS 24 h after transfection, then fixed with 4% paraformaldehyde in PBS for 20 min, and permeablized with acetone/methanol (1:1) for 15 min at room temperature. Fixed cells were blocked with 10% horse serum in PBS for 20 min and incubated with the appropriate antibody at a 1:200 dilution. The same blocking solution was used for washing before incubating with secondary antibodies. MitoTracker (Invitrogen) was used according to the manufacturer's instruction. Coverslips were mounted with Vectashield/Dapi (Vector Laboratories) and examined with a Nikon Eclipse E600 epifluorescence microscope.

Subcellular Localization by Differential Centrifugation. Harvested cells were washed two times with PBS and transferred to 1 mM *N*-2-hydroxyethylpiperazine-*N*′-2-ethanesulfonic acid (HEPES) buffer at pH 7.4 on ice for 5 min. Cells were then adjusted to 10 mM HEPES buffer at pH 7.4 containing 250 mM sucrose and homogenized with a Balch-style ball homogenizer (*24*). Subcellular fractions were collected by differential centrifugation, employing a modification of the method of Lutsenko and Cooper (*25*). Briefly, the P1 fraction containing unbroken cells and large cell fragments was obtained by centrifugation for 5 min at 500*g*; a P2 fraction containing mitochondria was obtained by centrifugation for 10 min at 3000*g*; and finally a P3 fraction containing other light vesicles was obtained by centrifugation for 45 min at 20 000*g*. The supernatant of the P3 fraction (S3) contains soluble proteins.

Electrophoresis and Immunoblot Analysis. SDS-PAGE was performed in a Bio-Rad Protean system following the

[1] Abbreviations: Abz, 2-aminobenzoyl; ANP, atrial natriuretic peptide; EDDnp, ethylenediamine-2,4-dinitrophenyl; Fmoc, 9-fluorenylmethoxycarbonyl; EST, expressed sequenced tag; GFP, green fluorescent protein; GRF, growth hormone releasing factor; MALDI-TOF, matrix assisted laser desorption ionization−time of flight.

protocol of Laemmli (*26*). Resolved proteins were then transferred according to Towbin et al. (*27*) onto a polyvinyldifluoride (PVDF-F) membrane (Millipore). CS presequence peptide was resolved in a 10−20% Tricine gel using an Xcell SureLock Mini-gel system (Invitrogen). Specific proteins were detected and quantified using a Li-COR Odyssey Imaging system. The BioRad Precision Plus All Blue Protein standard was used for estimating molecular weights of protein bands.

Protein Assay. Protein concentration was determined using Coomassie Plus (Pierce Chemical Company). Bovine serum albumin provided with the reagent was used as the protein standard.

In Vitro Translation and Processing. An MP1 cDNA and a mitochondrial CS cDNA (accession no. BC010106, obtained from Invitrogen) were subcloned into the pBluescript vector by PCR. Proteins were expressed using a coupled transcription/translation system (Promega) and radiolabeled with Tran [^{35}S] (20 μCi/50 μL; MP Biomedicals). For studying preprotein processing, the protocol of Cavadini et al. (*28*) was used except that the incubation temperature was 30 °C. Briefly, 1 μL of translation mixture was added to a reaction buffer containing 10 mM HEPES-KOH at pH 7.4, 1 mM dithiothreitol, 1 mM $MnCl_2$, 1 mM $ZnCl_2$, and varied amounts of processing enzymes. Processed products were analyzed by 10% SDS-PAGE and detected with a GE Typhoon system.

RESULTS

Kinetics. MP1 expressed in Sf9 cells is processed as evidenced by the finding that it exhibits a lower molecular weight than the enzyme derived from *E. coli* (Figure 1b). The latter form of MP1 was expressed as a fusion protein containing an internal TEV cleavage site such that cleavage by TEV generated the full-length unprocessed MP1 with two additional N-terminal amino acids. Furthermore the Sf9 form of MP1 was shown to have a mitochondrial localization by immunofluorescence (Figure 1c). For kinetic studies we used the mature processed enzyme.

Since MP1 was previously shown to cleave leumorphin at a monobasic site, we initially characterized the enzyme using two intramolecularly quenched substrates containing either a part of the leumorphin sequence (Abz-RRQFKV-VTRSQ-EDDnp) or a substrate containing a dibasic pair (Abz-YGGLRRGQ-EDDnp). The K_m and k_{cat} values for these substrates are nearly equivalent, being 1.07 μM and 4.8 min^{-1} for Abz-RRQFKVVTRSQ-EDDnp and 0.5 μM and 6.8 min^{-1} for Abz-YGGLRRGQ-EDDnp. The presence of one or two basic residues does not seem to affect the kinetics with these substrates.

We next studied the reaction of MP1 with a number of physiologically active peptides. The K_m for each peptide was determined by using it as an alternate substrate inhibitor of Abz-GGYRRGQ-EDDnp hydrolysis and thus would reflect primarily if not totally the intact peptide, while k_{cat} was determined from a linear initial rate at a saturating substrate concentration and it too would reflect reaction of the intact peptide. As shown in Table 1, MP1 exhibits a broad substrate specificity. There appears to be a trend that peptides containing 13 or more residues exhibit K_m values of 2 μM or less. Of the four peptides containing 11 or fewer residues that were studied, three exhibited K_m values above 10 μM. Similarly, peptides containing 13 or more residues exhibited k_{cat} values below 10 min^{-1}, while three of the four peptides containing 11 or fewer residues exhibited k_{cat} values above 30 min^{-1}. As a consequence k_{cat}/K_m values tend to vary little among substrates with the exception of human leumorphin and ANP, which exhibited the highest k_{cat}/K_m values. Of the substrates tested, insulin exhibited the lowest k_{cat}/K_m, because of its high K_m and low k_{cat} values.

Table 1: Kinetics of Hydrolysis of Physiological Peptides by MP1

peptide	peptide size (no. residues)	K_m[a] (μM)	k_{cat}[b] (min^{-1})	k_{cat}/K_m (M × min^{-1} × 10^5)
Leu-enkephalin	5	20.8 ± 0.9	39.0 ± 3.9	18.7 ± 2.1
bradykinin	9	16.2 ± 0.8	35.4 ± 0.9	21.8 ± 1.2
angiotensin I	10	1.7 ± 0.1	7.6 ± 0.4	44.6 ± 4.3
substance P	11	13.8 ± 1.0	32.7 ± 2.6	23.6 ± 2.5
dynorphin B	13	1.9 ± 0.2	8.9 ± 0.1	46.3 ± 6.8
dynorphin A	17	0.8 ± 0. 1	4.8 ± 0.4	62.6 ± 6.8
endothelin 1	21	0.7 ± 0.1	1.1 ± 0.0	15.8 ± 4.6
somatostatin	28	0.1 ± 0.0	0.6 ± 0.0	41.7 ± 3.8
ANP	28	0.2 ± 0.0	4.5 ± 0.4	199.2 ± 18.6
leumorphin (human)	29	0.4 ± 0.0	5.9 ± 0.4	140.6 ± 10.7
leumorphin (porcine)	29	0.8 ± 0.0	4.9 ± 0.2	63.5 ± 4.5
β-endorphin	31	0.9 ± 0.0	5.8 ± 0.1	62.6 ± 5.1
calcitonin	32	2.4 ± 0.0	3.8 ± 0.1	15.4 ± 0.6
β-amyloid (1−40)	40	1.7 ± 0.1	3.3 ± 0.1	19.5 ± 1.1
GRF	40	0.5 ± 0.0	1.4 ± 0.1	29.4 ± 3.4
insulin	51	54.5 ± 5.5	0.2 ± 0.0	0.03 ± 0.00

[a] K_m values were determined by using the indicated peptide as an alternate substrate inhibitor of 2.2 μM Abz-GGFYRRVGQ-EDDnp hydrolysis (K_m = 1.07 μM). Under the assay conditions employed, little if any of the inhibitory peptide would have been cleaved. [b] Since most peptides are cleaved at multiple sites, k_{cat} could reflect cleavages at more than one site.

Cleavage Sites. MP1 dependent peptide cleavage products were isolated by HPLC and identified by mass spectrometry. This analysis showed that MP1 cleaved at multiple sites within its peptide substrates and that some products which appear to be derived from the intact peptide, as judged by identification of both N- and C-terminal fragments, appeared at latter time points. In addition the secondary cleavage of some initial products was evident based on the analysis of product appearance as a function of time. For example, in the case of β-endorphin, MP1 initially cleaves this peptide at Ala^{21}-Ile^{22} generating fragments YGGFMTSEKSQT-PLVTLFKNA (b, Figure 2) and IIKNAYKKGE. The latter peptide was identified near the void volume of the column (not shown). Fragment b is subsequently cleaved by MP1 at Gly^3-Phe^4 at the N-terminal region generating FMTSEK-SQTPLVTLFKNA (c, Figure 2). We also found that MP1 acts on FMTSEKSQTPLVTLFKNA (fragment c) by removing the N-terminal Phe (F). Additionally, MP1 cleaves the C-terminal region of fragment c at Leu^{17}-Phe^{18}, Thr^{16}-Leu^{17}, and to a lesser extent Pro^{13}-Leu^{14} and Leu^{14}-Val^{15}.

One of the substrates of MP1, dynorphin 29, also called leumorphin (YGGFLRRQFKVVTRSQQDPNAYSGQLF-DA), was reported to be cleaved at the T−R bond generating dynorphin B and dynorphin 14−29 (*17*). Although we indeed detected the MP1 dependent cleavage of porcine dynorphin 29 at the T−R bond (Table 2), this turned out to be a minor cleavage site as it was not observed until latter time points. Instead the initial cleavage sites were at D^{18}-P^{19} and L^{26}-F^{27}. On the other hand, the initial cleavage site of human dynorphin 29, which differs by five residues (E17 = Q, Y22 = S, E23 = G, E24 = Q, and V29 = A), is at the T−R bond, showing the influence of C-terminal residues on the

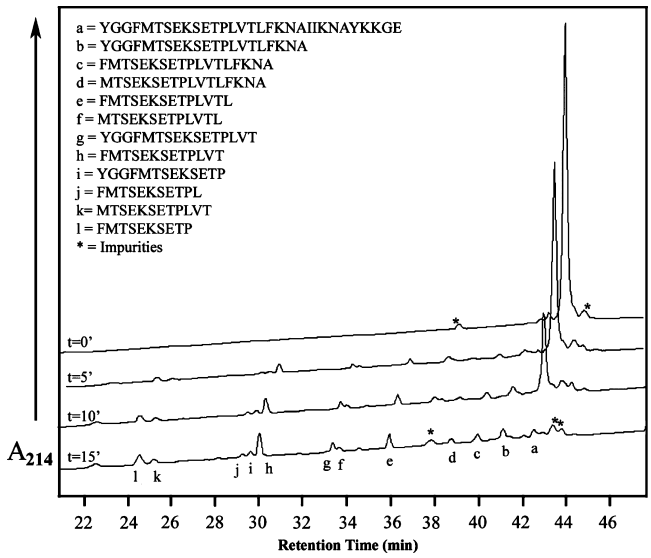

FIGURE 2: HPLC chromatogram of the β-endorphin and its fragments produced by hydrolysis by MP1. The β-endorphin (30 μM) was cleaved by 2 μg of MP1 for the indicated time in 25 mM Tris buffer at pH 7.5. The reaction was stopped by the addition of trichloroacetic acid to 0.1% and subjected to reverse phase HPLC on a Vydac C_4 column as previously described (*5*). Peaks were collected manually and subjected to mass spectral analysis for identification.

Table 2: Cleavage Sites of Human Pitrilysin MP1 on Physiological Peptides[a]

peptide	cleavage sites
angiotensin I	DRVY▼IHP▼FHL
ANP	SLRRSSCFGGRMD▼RIGAQSGLGCNS▼FRY
bradykinin	RPPG▼FSPFR
calcitonin	CGNLSTC▼MLG▼TYTQDFNK↓FHTFPQTAIGVGAP
dynorphin A	Y↓GGFLRR↓IRP▼KLKWDNQ
dynorphin B	Y↓GGFLRRQF↓K▼VVT
GRF	Y↓ADAIFTNSYRKVLG▼QLS▼ARKL↓QDIMQQGESNQERGA
Leu-enkephalin	Y▼GGFL
leumorphin (human)	Y↓GGFLRRQF↓K▼VVT▼RSQQDPNAYSGQLFDA
leumorphin (porcine)	Y↓GGFLRRQFK↓VVT↓RSQED▼PNAYYEEL▼FDV
substance P	RPKPQQF↓FG▼LM
β-amyloid (1−40)	DAEFRHDSGYEVHHQKLVFF▼AEDVGSNKGAIIGL↓MVGGVV
β-endorphin	YGG↓F↓MTSEKSETPLV↓T↓L▼FKNA▼IIKNAYKKGE

[a] Peptide hydrolysis was followed at several time points to determine initial and secondary or slower cleavage sites. Filled triangles indicate initial cleavage sites, while arrows indicate secondary cleavage sites that were either derived from initial products or appeared at latter time points.

cleavage site. This may also reflect differences in conformation of the bound peptide. The product dynorphin B was subsequently hydrolyzed at the K−V, F−K, and Y−G sites, which are the same cleavages observed when dynorphin B was the substrate.

As noted in the reaction with Leu-enkephalin, MP1 was able to cleave an N-terminal tyrosine, which was also detected in the reactions with dynorphin B, dynorphin A, and GRF (Table 2) and as noted above an N-terminal Phe. Judging from the cleavage products listed in Table 2, it is unlikely that this activity can be attributed to contamination by an aminopeptidase since only an N-terminal Tyr or Phe was cleaved. However, to rule out aminopeptidase activity we carried out the hydrolysis of β-endorphin, dynorphin A, and leumorphin in the presence of 10 μM bestatin, a broad spectrum aminopeptidase inhibitor. We observed no effect

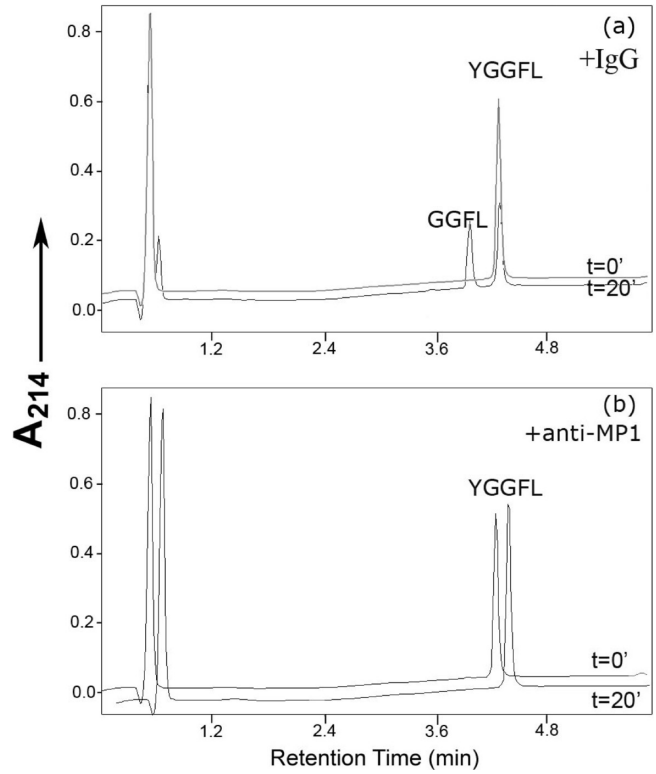

FIGURE 3: MP1 can cleave an N-terminal tryosine residue. Leu-enkephalin (500 μM) was cleaved by 1 μg of MP1 in 25 mM phosphate buffer at pH 7.5. The reaction was stopped and analyzed by reverse phase HPLC as described in Figure 2. Peaks were identified by comparison to authentic standards. Upper panel: MP1 incubated with rabbit IgG on ice for 1 h was then absorbed with protein A Sepharose. Lower panel: MP1 incubated with anti-MP1 on ice for 1 h and then absorbed with protein A Sepharose.

on the rate of peptide hydrolysis or the distribution of cleavage products. Additionally, we used an anti-MP1 antibody to immunodeplete MP1 and measure the reaction of the immunodepleted sample with Leu-enkephalin (YGGFL). As the Y−G bond is the only cleavage in Leu-enkephalin, it is clear that elimination of MP1 by immunodepletion effectively eliminated the N-terminal cleavage activity toward Leu-enkephalin (Figure 3).

Since MP1 can cleave a peptide at multiple sites and secondary cleavages were demonstrated, we focused on the initial cleavage sites and some notable secondary cleavages as shown in Table 2. Examination of the residues at the P1′ and P1 sites (based on the nomenclature of Schechter and Berger (*29*)) did not reveal a clear pattern of cleavage preference for a particular residue. However, two cleavage patterns were observed. The first became apparent when the cleavage sites were aligned. Here we note that many, but not all, of the cleavage sites occur two to five residues C-terminal to an arginine residue, Table 3. This resembles the cleavage preference of mitochondrial processing protease (MPP). Another cleavage preference is seen at the amino side of Phe when it is located within three to five residues to the C-terminus. Examples in Table 2 are angiotensin I, ANP, bradykinin, porcine leumorphin, and β-endorphin (fragment c conversion to fragment e, Figure 2).

Since one of the cleavage patterns of MP1 resembles that of the mitochondrial processing protease, we determined whether or not MP1 is able to actually process a mitochon-

Table 3: MP1 Cleavage Patterns

MP1 Cleavage Motifs Mimic That of Mitochondrial Processing Proteases

peptide	cleavage alignment	motif
angiotensin I	D**R**VY▾IHPFHL	R-3
ANP	RRSSCFGG**R**MD▾RIGAQSGLGCNSFRY	R-3
bradykinin	**R**PPG▾FSPFR	R-4
dynorphin A	YGGFL**RRIR**P▾KLKWDNQ	R-2, R-4, or R-5
dynorphin B	YGGFL**RR**QF▾KVVT	R-3 or R-4
dynorphin B	YGGFL**RR**QFK▾VVT	R-4 or R-5
GRF	...QLSA**R**KL▾LQDIMSRQQGESNQE	R-3
GRF	IFTNSY**R**KVLG▾QLS	R-5

Primary Cleavage Sites That Did Not Contain an R-2 to R-5 Motif

peptide	cleavage site
calcitonin	CNS▾FRY
calcitonin	STC▾MLG
ANP	MLG▾TYT
Leu-enkephalin	Y▾GGFL
β-amyloid 1−40	VFF▾A
β-endorphin	KNA▾IIK

drial precursor protein. We tested radiolabeled in vitro translated full-length CS, which contains the presequence MALLTAAARLFGAKNASCLVLAARHAS as a substrate. In the presence of 0.2 μg of yMPP, full-length CS is processed to its mature form within a 2 h incubation period, Figure 4. However, MP1 did not generate mature CS even with a five times higher amount of enzyme (1 μg) and longer incubation time (4 h), suggesting it does not behave as a protein processing enzyme but rather a true peptidase cleaving peptides, not proteins.

To determine whether MP1 could be involved in the clearance of presequence peptides we synthesized the CS presequence peptide and tested it as a substrate for MP1. As shown in Figure 5a, MP1 can in fact cleave the presequence peptide. We determined the kinetic parameters for this 27-amino acid peptide and observed a K_m of 0.17 μM, a k_{cat} of 1.1 min^{-1}, and a k_{cat}/K_m of 6.7 × 10^5 M min^{-1}. The cleavage sites were also determined using mass spectrometry to detect peptide fragments generated by MP1 cleavage (Figure 5b). Only the initial cleavage sites are shown in this figure. In each case both the N- and the C-terminal complementary fragments were identified, showing that MP1 cleaves primarily at sites in the middle of the peptide.

Effects of Metal Ions. AtPreP, the plant homologue of MP1, requires Mg^{2+} or Ca^{2+} for full activity. We thus examined the effect of metal ions on MP1 activity. As shown in Table 4, the enzyme is inhibited by nickel and zinc and slightly activated by manganese, which parallels the effect observed with nardilysin (*39*). Other metals were without effect.

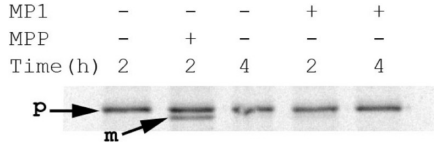

FIGURE 4: Pre-CS is processed by yMPP but not by MP1. The mitochondrial precursor form of CS was generated by in vitro translation in the presence of ^{35}S Met/Cys. From this translation mixture 1 μL was incubated with MP1 (1 μg) or yMPP (0.2 μg) and then analyzed by SDS-PAGE. P = precursor form; M = mitochondrial processed form.

Table 4: Effect on Metal Ions on hMP1

salt	% activity remaining[a]
$CaCl_2$, 1 mM	98 ± 0
KCl, 2 mM	77 ± 1.9
$MgCl_2$, 1 mM	102 ± 0.9
$MnCl_2$, 1 mM	143 ± 6.5
NaCl, 2 mM	83 ± 0
$NiCl_2$, 1 mM	18 ± 2.8
$ZnCl_2$, 1 mM	0

[a] MP1 was diluted in 20 mM Tris-HCl at pH 7.5 in the presence of metal salts at the concentration indicated. MP1 activity was assayed in duplicate with 2.7 μM Abz-YGGLRRGQ-EDDnp as substrate under the same conditions. Experiments were conducted in duplicates, and average values are presented with the range given.

Subcellular Localization. To determine the subcellular localization of MP1, we employed two approaches, namely, differential centrifugation and immunocytochemistry in a neuronal NT2 cell line and in a non-neuronal HepG2 cell line. Differential centrifugation showed that MP1 is enriched in the pellet derived from centrifugation at 3000*g* (P2 fraction) and cosediments with mMDH (Figure 6). Although not shown, fractionation of HepG2 cells produced the same result. Sonication of the P2 fraction released the enzyme demonstrating that MP1 is in the soluble fraction of the mitochondrion in HepG2 cells. MP1 was also shown to colocalize with the soluble mitochondrial protein mMDH by immunocytochemistry (Figure 7).

The first 15 amino acids of MP1 contain basic and hydrophobic residues organized in groups when this sequence is analyzed on a helical wheel, suggesting this region might contain a mitochondrial targeting signal. To determine whether or not this presequence actually contains a functional mitochondrial-targeting signal, a truncation mutant MP1Δ15 was constructed. Additionally, as a 22- (*30*) or 29-amino acid (*31*), long presquences are predicted to be cleaved during the translocation process; we also constructed another 38-residue truncation mutant (MP1Δ38) to ensure that the putative target signal is completely removed. We found that both of these truncation mutants, when expressed in NT2 or HepG2 cells, are mislocalized to cytoplasmic compartments and the nucleus. This is shown in Figure 7 for MP1Δ15. Next, we generated a construct in which the N-terminal 15-amino acid putative MP1 mitochondrial targeting sequence (MWRCGGRRGLCVLRR-) was fused to GFP. When trans-

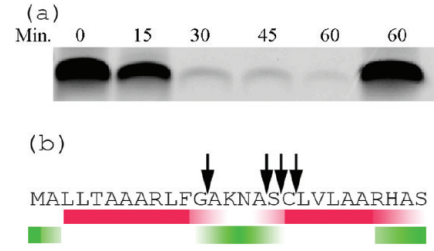

FIGURE 5: MP1 cleaves the presequence peptide of CS. (a) The reaction mixture contained 3.6 μg of purified MP1 and 8.6 μg of peptide in 50 mM Tris-HCl buffer at pH 7.5. The molar ratio of enzyme to peptide was 1:100. Aliquots were removed at the times indicated and analyzed on a 10−20% Tricine gel stained with Coomassie blue. The last lane to the right shows a peptide-alone control. (b) Cleavage sites were determined by detecting peptide fragments in the reaction mixture by mass spectrometry. Secondary structure was predicted with the Prof Prediction program (www.proteinpredict.org). Helical structures are showed in red and random coil in green.

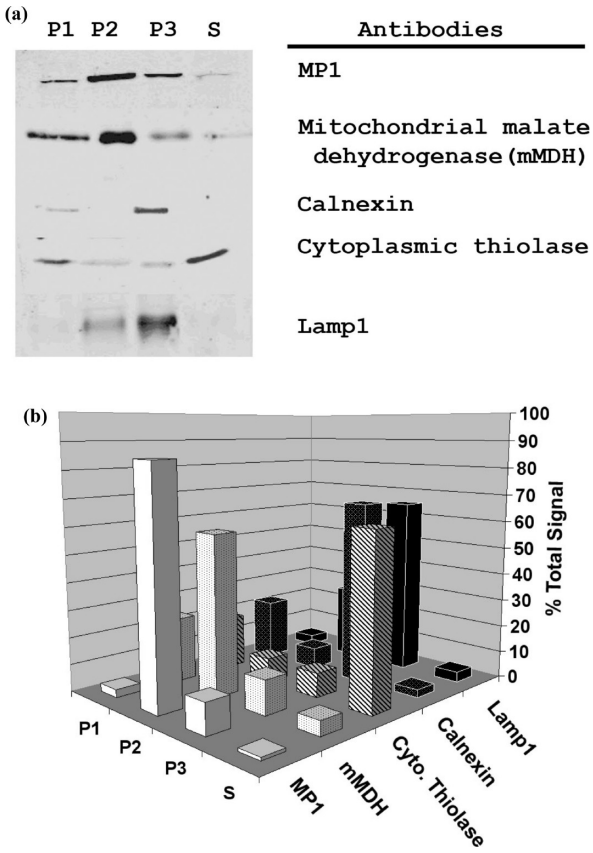

FIGURE 6: Subcellular localization of MP1. NT2 cells were fractionated by differential centrifugation as described in Experimental Procedures. (a) A 30 μg portion of protein from each subcellular fraction was analyzed by Western blotting. The antibodies used are shown at the right column of the blots. (b) The intensities of the bands representing the fluorescence signal of each antibody were calculated from the data in part a and expressed relative to the total fluorescence for each antibody.

fected into NT2 or HepG2 cells this construct produced mitochondrial GFP, Figure 8.

DISCUSSION

In this study we have examined the properties of mammalian pitrilysin MP1 in terms of its intracellular targeting and its substrate specificity. Although other metallopeptidases of the inverzincin family localize to both the cytosol and the mitochondria (i.e., insulysin (*32*) and neurolysin (*33*)), we demonstrate here that MP1 is primarily, if not exclusively, a mitochondrial protein with its mitochondrial targeting signal sequence located within a 15-residue presequence (MWRCGGRRGLCVLRR). Removal of this presequence mislocalizes MP1 in cells, while this sequence is sufficient to target a nonmitochondrial protein (GFP) into mitochondria. It is generally accepted that mitochondrial presequences are amphipathic helices in which basic and hydrophobic residues are localized to different sides on a helical cylinder (*34*), suggesting an initial interaction with multiple proteins at the mitochondrial membrane. In the case of the presequence of MP1, Arg residues at positions 3, 7, and 14 can be clustered on the same side of a helical wheel. Interestingly, MP1 exists as two variants. The MP1 clone (accession no. BC005025) used in the present study contains an Arg in the eighth position. There is a more predominant variant containing Gln at this position due to a variation of the eighth codon CGG (^{8}Arg) versus CAG (^{8}Gln). The ^{8}Arg variant exists at a frequency of ~20% based on 100 EST clones examined. However, it is likely that ^{8}Arg is not important in mitochondrial targeting since it faces away from the basic cluster. The MP1 mitochondrial sequence is functionally conserved, as mammalian MP1 is targeted to insect mitochondria.

MP1 was initially described as a metallopeptidase cleaving the opioid peptide leumorphin, but its specificity was not investigated. We have further characterized MP1 with a series of opioid and other bioactive peptides that have been studied as substrates for other metallopeptidases. MP1 generally exhibits a preference for peptides of 13 or more amino acids in terms of lower K_m values, while k_{cat} values show an inverse relationship with peptides of 13 or more amino acids exhibiting lower k_{cat} values. Although the structure of MP1 has not been determined, it exhibits 54% sequence similarity (30% sequence identity) to insulysin, suggesting it has a similar structure. The long extended substrate-binding site of insulysin, if conserved in MP1, would account for the lower K_m values generally seen with larger peptides. At the same time these extended interactions may contribute to the lower k_{cat} values if product dissociation or opening of a closed conformation were rate limiting.

There are, however, exceptions in terms of the trends observed between substrate size and K_m. Most notable is insulin with its two chains linked by disulfide bonds. It may be too large to optimally fit into the active site of MP1. Another exception is angiotensin I which is a 10-residue peptide that has a lower K_m and a lower k_{cat} than other similar-sized peptides. This apparent anomaly likely reflects a sequence that interacts favorably with the active site.

When comparing the residues at the P1 and P1′ cleavage sites of physiological peptides, the cleavage preference of MP1 appears unique as it does not follow any known pattern of other inverzincins. For example, insulysin prefers hydrophobic or basic residue at either the amino side (*35*) or the carboxyl side (*36*) of the scissile bond. PreP, a plant homologue of MP1, prefers P1 to be a basic residue and P1′ to be uncharged residue (*18*). However, P1 can be a basic, acidic, small, or hydrophobic residue for MP1. Two consequences result from these differences. First, MP1 shares substrates but not cleavage sites with other inverzincins. For example, except for the T−R bond in leumorphin, there are no overlapping cleavage sites for this substrate between bacterial pitrilysin (*37*) and MP1. Second, MP1 exhibits even broader substrate specificity than other M16 metallopeptidases. This is exemplified by the fact that angiotensin I and bradykinin are not cleaved by protease III (*37*), insulysin (*38*), or nardilysin (*39*) but are substrates of MP1. Additionally, the ability to cleave an N-terminal Phe or Tyr residue is unique to MP1.

It is noted that the multiple cleavage sites for MP1 within the CS presequence peptide are clustered in the middle of the peptide. Structural analysis predicts that this central region is an unstructured one, flanked by two helical structure regions of the peptide. Thus, in this case the open accessibility of this central region could contribute as a cleavage site determinant.

Solely on the basis of its mitochondrial localization, MP1 has been postulated to be a peptidase that clears free presequences inside the mitochondria (*20*). We have provided

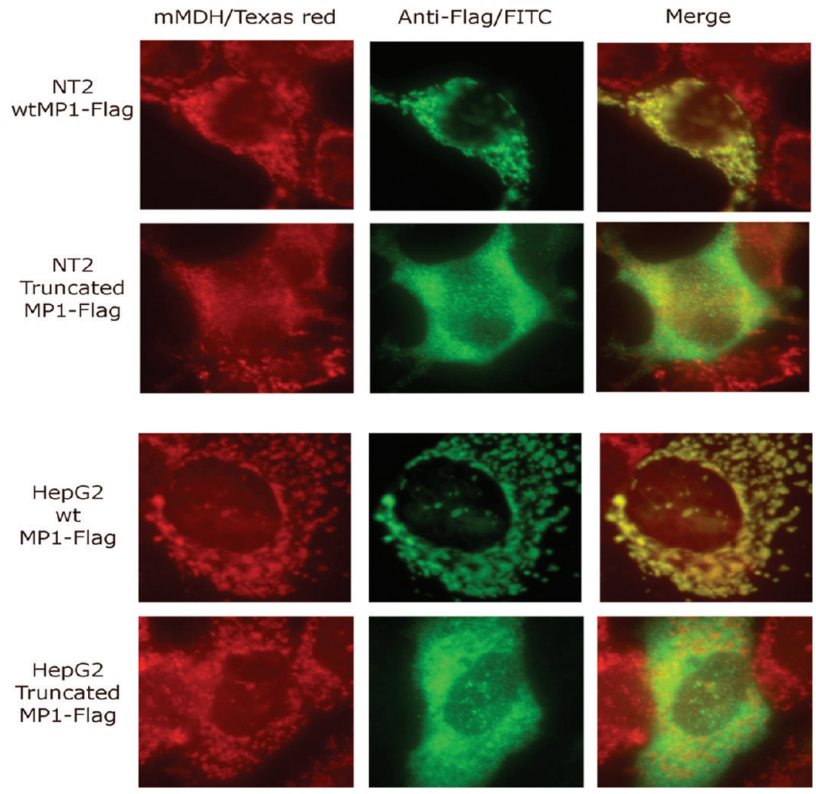

FIGURE 7: Subcellular localization of MP1 in NT2 and HepG2 cells. NT2 or HepG2 were transfected with either a full-length Flag tagged MP1 (wtMP1-Flag) or an N-terminal truncated MP1-Flag. After a 24 h culture, cells were fixed and probed with rabbit anti-mMDH and mouse anti-Flag (see Experimental Procedures).

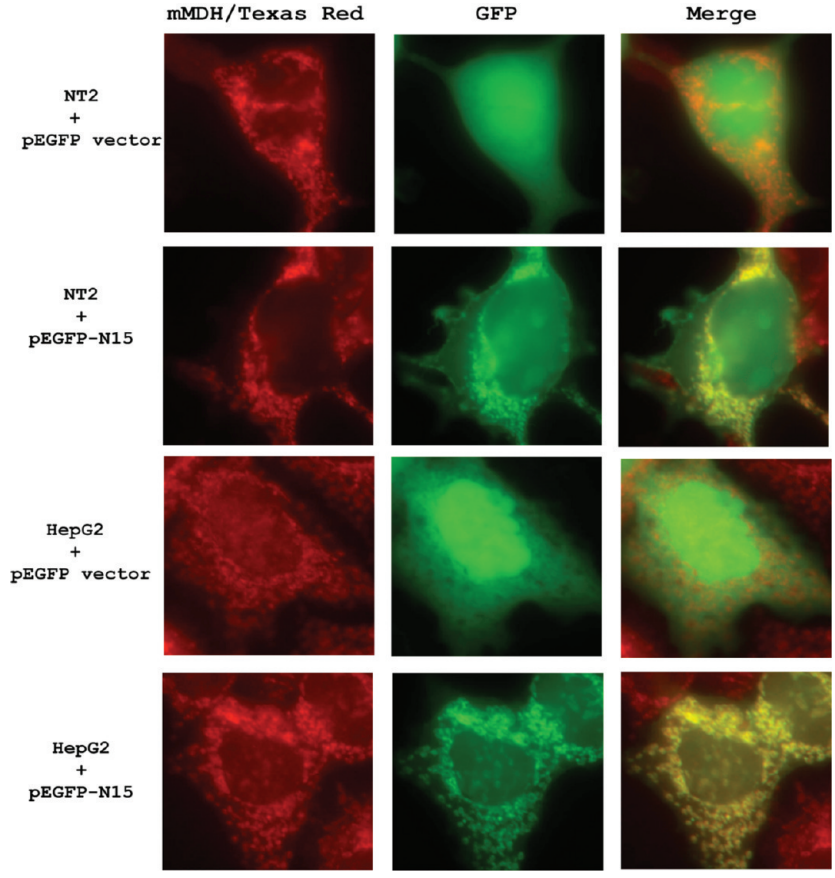

FIGURE 8: N-terminal sequence of MP1 targets GFP to mitochondria. NT2 and HepG2 cells were transfected with a GFP expression vector to which a 15-residue N-terminal MP1 is fused (pEGFP-N15). Cells were incubated for 24 h and then stained and imaged as described in Experimental Procedures.

in vitro evidence that MP1 can in fact degrade a mitochondrial presequence peptide, that of mammalian CS. The cleavage of the CS presequence exhibited similar kinetics to other peptides examined, indicating that MP1 is indeed a potential candidate for such a function. If in fact MP1 functions to hydrolyze released mitochondrial presequence peptides, then its broad substrate specificity may serve this function well, as mitochondrial presequence peptides are rather diverse in their sequences. In the yeast intermembrane space, a metallopeptidase MoP112 (*40*) belonging to the M16 pitrilysin family has recently been shown to cleave peptides along with another metallopeptidase saccharolysin (PRD1). Presequence peptides were detected in the double mutant Δ*mop112*Δ*prd1* but not found in wild type yeast. Interestingly, although fewer presequences were detected in mutants of either Δ*mop112* or Δ*prd1*, the identity of these peptides differed, indicating that these two enzymes have overlapping but not identical specificity. It is tempting to speculate that MP1 may serve a similar function as MoP112 or PRD1 in mammalian mitochondria.

On the basis of the ability of MP1 to degrade a number of physiological peptides, it is also likely that the enzyme may degrade other peptides in the mitochondria. Besides presequence peptides, mitochondrial peptides are derived from the degradation of misfolded proteins by adenosine triphosphate (ATP)-dependent proteases in the inner mitochondrial membrane (*41*). These peptides are subsequently either degraded by oligopeptidases or exported out of the mitochondria.

ACKNOWLEDGMENT

We thank NIDA for providing dynorphin B and β-endorphin through NeoMPS, Inc. We would also like to thank Drs. Sydney Whiteheart and Becky Dutch for technical advice on immunochemistry and radiolabeling experiments, respectively. We thank Dr. Carol Beach for conducting the mass spectrometry analysis at the University of Kentucky Proteomics Core facility, which is supported in part by the National Center for Research Resources Grant P20RR02017.

REFERENCES

1. Hooper, N. M. (1994) Families of zinc metalloproteases. *FEBS Lett. 345*, 1–6.
2. Finch, P. W., Wilson, R. E., Brown, K., Hickson, I. D., and Emmerson, P. T. (1979) Complete nucleotide sequence of the *Escherichia coli* gene encoding protease III. *Nucleic Acids Res. 14*, 7695–7703.
3. Rawlings, N. D., Morton, F. R., and Barrett, A. J. (2006) MEROPS: the peptidase database. *Nucleic Acids Res. 34*, D270–D272.
4. Shen, Y., Joachimiak, A., Rosner, M. R., and Tang, W. J. (2006) Structures of human insulin-degrading enzyme reveal a new substrate recognition mechanism. *Nature 443*, 870–874.
5. Chow, K. M., Csuhai, E., Juliano, M. A., Pyrek, J. S., Juliano, L., and Hersh, L. B. (2000) Studies on the subsite specificity of rat nardilysin (N-arginine dibasic convertase). *J. Biol. Chem. 275*, 19545–19551.
6. Hersh, L. B. (2003) Peptidases, proteases and amyloid beta-peptide catabolism. *Curr. Pharm. Des. 9*, 449–454.
7. Qiu, W. Q., and Folstein, M. F. (2006) Insulin, insulin-degrading enzyme and amyloid-beta peptide in Alzheimer's disease: review and hypothesis. *Neurobiol. Aging 2*, 190–198.
8. Sarada, B., Thiele, D., Dang, T., Safavi, A., Hersh, L. B., and Cottam, G. L. (1997) Increased expression of an endopeptidase (gamma-EGE/IDE) hydrolyzing beta-endorphin during differentiation and maturation of bone marrow macrophages. *J. Leukocyte Biol. 62*, 753–760.
9. Sarada, B., Thiele, D., Dang, T., Lee, J., Safavia, A., Hersh, L. B., and Cottam, G. L. (1998) Anti-CD3 activation of human CD4+ T cells increases expression of the intracellular beta-endorphin endopeptidase (IDE/gamma-EpGE). *J. Neuroimmunol. 85*, 59–68.
10. Chesneau, V., Prat, A., Segretain, D., Hospital, V., Dupaix, A., Foulon, T., Jegou, B., and Cohen, P. (1996) NRD convertase: a putative processing endoprotease associated with the axoneme and the manchette in late spermatids. *J. Cell Sci. 109*, 2737–2745.
11. Ma, Z., Wang, X., Hockman, S., Snow, E. C., and Hersh, L. B. (2005) Subcellular localization of nardilysin during mouse oocyte maturation. *Arch. Biochem. Biophys. 434*, 187–194.
12. Chow, K. M., Ma, Z., Cai, J., Pierce, W. M., and Hersh, L. B. (2005) Nardilysin facilitates complex formation between mitochondrial malate dehydrogenase and citrate synthase. *Biochim. Biophys. Acta 1723*, 292–301.
13. Nishi, E., Prat, A., Hospital, V., Elenius, K., and Klagsbrun, M. (2001) N-arginine dibasic convertase is a specific receptor for heparin-binding EGF like growth factor that mediates cell migration. *EMBO J. 20*, 3342–3350.
14. Stricker, R., Chow, K. M., Walther, D., Hanck, T., Hersh, L. B., and Reiser, G. (2006) Interaction of the brain-specific protein p42IP4/centaurin-alpha1 with the peptidase nardilysin is regulated by the cognate ligands of p42IP4, PtdIns(3,4,5)P3 and Ins(1,3,4,5)P4, with stereospecificity. *J. Neurochem. 98*, 343–354.
15. Ito, A. (1999) Mitochondrial processing peptidase: Multiple-site recognition of precursor proteins. *Biochem. Biophys. Res. Commun. 265*, 611–616.
16. Gakh, O., Cavadini, P., and Isaya, G. (2002) Mitochondrial processing peptidases. *Biochim. Biophys. Acta 1592*, 63–77.
17. Mzhavia, N., Berman, Y. L., Qian, Y., Yan, L., and Devi, L. A. (1999) Cloning, expression, and characterization of human metalloprotease 1: a novel member of the pitrilysin family of metalloendoproteases. *DNA Cell Biol. 18*, 369–380.
18. Ståhl, A., Nilsson, S., Lundberg, P., Bhushan, S., Biverståhl, H., Moberg, P., Morisset, M., Vener, A., Mäler, L., Langel, U., and Glaser, E. (2005) Two novel targeting peptide degrading proteases, PrePs, in mitochondria and chloroplasts, so similar and still different. *J. Mol. Biol. 349*, 847–860.
19. Taylor, S. W., Fahy, E., Zhang, B., Glenn, G. M., Warnock, D. E., Wiley, S., Murphy, A. N., Gaucher, S. P., Capaldi, R. A., Gibson, B. W., and Ghosh, S. S. (2003) Characterization of the human heart mitochondrial proteome. *Nat. Biotechnol. 21*, 281–286.
20. Falkevall, A., Alikhani, N., Bhushan, S., Pavlov, P. F., Busch, K., Johnson, K. A., Eneqvist, T., Tjernberg, L., Ankarcrona, M., and Glaser, E. (2006) Degradation of the amyloid beta -protein by the novel mitochondrial peptidasome, PreP. *J. Biol. Chem. 281*, 29096–29104.
21. Suemizu, H., Aiba, K., Yoshikawa, T., Sharov, A. A., Shimozawa, N., Tamaoki, N., and Ko, M. S. (2003) Expression Profiling of Placentomegaly Associated with Nuclear Transplantation of Mouse ES Cells. *Dev. Biol. (San Diego, CA, U.S.) 253*, 36–53.
22. Gakh, O., Obsil, T., Adamec, J., Spizek, J., Amler, E., Janata, J., and Kalousek, F. (2001) Substrate binding changes conformation of the alpha-, but not the beta-subunit of mitochondrial processing peptidase. *Arch. Biochem. Biophys. 385*, 392–396.
23. Kapust, R. B., Tözsér, J., Fox, J. D., Anderson, D. E., Cherry, S., Copeland, T. D., and Waugh, D. S. (2001) Tobacco etch virus protease: Mechanism of autolysis and rational design of stable mutants with wild-type catalytic proficiency. *Protein Eng. 14*, 993–1000.
24. Chen, D., Xu, W., He, P., Medrano, E. E., and Whiteheart, S. W. (2001) Gaf-1, a gamma -SNAP-binding protein associated with the mitochondria. *J. Biol. Chem. 276*, 13127–13135.
25. Lutsenko, S., and Cooper, M. J. (1998) Localization of the Wilson's disease protein product to mitochondria. *Proc. Natl. Acad. Sci. U.S.A. 95*, 6004–6009.
26. Laemmli, U. K. (1970) Cleavage of structural proteins during the assembly of the head of bacteriophage T4. *Nature 227*, 680–685.
27. Towbin, H., Staehelin, T., and Gordon, J. (1979) Electrophoretic transfer of proteins from polyacrylamide gels to nitrocellulose sheets: procedure and some applications. *Proc. Natl. Acad. Sci. U.S.A. 76*, 4350–4354.
28. Cavadini, P., Gakh, O., and Isaya, G. (2002) Protein import and processing reconstituted with isolated rat liver mitochondria and recombinant mitochondrial processing peptidase. *Methods 26*, 298–306.

29. Schechter, I., and Berger, A. (1967) On the size of the active site in proteases. I. Papain. *Biochem. Biophys. Res. Commun. 27*, 157–162.
30. Bendtsen, J. D., Nielsen, H., von Heijne, G., and Brunak, S. (2004) Improved prediction of signal peptides: SignalP 3.0. *J. Mol. Biol. 340*, 783–795.
31. Claros, M. G., and Vincens, P. (1996) Computational method to predict mitochondrially imported proteins and their targeting sequences. *Eur. J. Biochem. 241*, 779–786.
32. Leissring, M. A., Farris, W., Wu, X., Christodoulou, D. C., Haigis, M. C., Guarente, L., and Selkoe, D. J. (2004) Alternative translation initiation generates a novel isoform of insulin-degrading enzyme targeted to mitochondria. *Biochem. J. 383*, 439–446.
33. Kato, A., Sugiura, N., Saruta, Y., Hosoiri, T., Yasue, H., and Hirose, S. (1997) Targeting of endopeptidase 24.16 to different subcellular compartments by alternative promoter usage. *J. Biol. Chem. 272*, 15313–15322.
34. Roise, D., and Schatz, G. (1988) Mitochondrial presequences. *J. Biol. Chem. 263*, 4509–4511.
35. Song, E. S., Mukherjee, A., Juliano, M. A., Pyrek, J. S., Goodman, J. P., Jr., Juliano, L., and Hersh, L. B. (2001) Analysis of the subsite specificity of rat insulysin using fluorogenic peptide substrates. *J. Biol. Chem. 276*, 1152–1155.
36. Mueller, D., Schulze, C., Baumeister, H., Buck, F., and Richter, D. (1992) Rat insulin-degrading enzyme: cleavage pattern of the natriuretic peptide hormones ANP, BNP, and CNP revealed by HPLC and mass spectrometry. *Biochemistry 31*, 11138–11143.
37. Cornista, J., Ikeuchi, S., Haruki, M., Kohara, A., Takano, K., Morikawa, M., and Kanaya, S. (2004) Cleavage of various peptides with pitrilysin from Escherichia coli: kinetic analyses using beta-endorphin and its derivatives. *Biosci., Biotechnol., Biochem. 68*, 2128–2137.
38. Safavi, A., Miller, B. C., Cottam, L., and Hersh, L. B. (1996) Identification of gamma-endorphin-generating enzyme as insulin-degrading enzyme. *Biochemistry 35*, 14318–14325.
39. Csuhai, E., Safavi, A., and Hersh, L. B. (1995) Purification and characterization of a secreted arginine-specific dibasic cleaving enzyme from EL-4 cells. *Biochemistry 34*, 12411–12419.
40. Kambacheld, M., Augustin, S., Tatsuta, T., Stefan Muller, S., and Langer, T. (2005) Role of the Novel Metallopeptidase MoP112 and Saccharolysin for the Complete degradation of Proteins Residing in Different Subcompartments of Mitochondria. *J. Biol. Chem. 280*, 20132–20139.
41. Leonhard, K., Herrmann, J. M., Stuart, R. A., Mannhaupt, G., Neupert, W., and Langer, T. (1996) AAA proteases with catalytic sites on opposite membrane surfaces comprise a proteolytic system for the ATP-dependent degradation of inner membrane proteins in mitochondria. *EMBO J. 15*, 4218–4229.

BI8016125